• Metabolomics • LC-MS • CRC Organoids/Microphysiological Systems

Exploring Metabolites within Organoids and Organoids-on-Chips during Colorectal Cancer (CRC) Therapeutic Treatments.

Ethan Canfield[1]; Ah Young Yoon[1], Carly Strelez[1]; Rachel Perez[1]; Aaron Schatz[1]; Heinz-Josef Lenz[2]; Jonathan Katz[1,2]; Shannon Mumenthaler[1,2,3]

[1] Ellison Institute of Technology, Los Angeles, CA
[2] Department of Medicine/Oncology, Keck School of Medicine, University of Southern California, Los Angeles, California
[3] Department of Biomedical Engineering, Viterbi School of Engineering, University of Southern California, Los Angeles, California

Correspondence: jkatz@eit.org
Reprints: https://reprints.katzlab.org/

Introduction

Organoids and microphysiological systems ("organoid-on-chip", OOC) represent methodologies to better recapitulate biological processes involved in diseases and their respective treatment modalities, overcoming some limitations with conventional tissue culture while not requiring the complexity of an animal model. We have coupled liquid chromatography-mass spectrometry (LC-MS) based untargeted metabolomics workflows to our cell culture-based models of colorectal cancer (CRC) to study the metabolic profiles of patient-derived organoids and OOCs in response to standard of care therapies. Effluent from the epithelial and endothelial compartments of the OOC model were compared across treatment conditions to examine changes induced by common CRC chemotherapeutics. This, collectively, provides a patient-specific view on drug disease interactions.

Beyond the use of mass spectrometry in the study of the biology of the system, mass spectrometry played a key role in validating the workflow and treatment conditions used by our partner biologists.

Highlights

- **Mass spectrometry based validation of OOC drug treatment experimental parameters**
- **High reproducibility observed in OOC effluent analyses**
- **Use of MassHunter Explorer greatly improved our ease of use and speed in data analysis.**

Evaluation Strategy

Individual CRC organoids and OOCs were treated with different chemotherapies, such as SN-38 (the active metabolite of irinotecan), 5-fluorouracil (5FU), and staurosporine (STA) (a pan-kinase inhibitor, as a positive control). Effluent samples from the microfluidic OOC (30 uL/h) were collected at various time points over a 6-day treatment period. One set of OOC and organoids was also maintained with untreated media. After collection, samples were frozen and stored at -80 °C. Once the treatment period concluded, cell pellets/lysed cells were also collected for testing. Metabolites were extracted using methanol and water, dried and resuspended in acetonitrile and water prior to analysis using HILIC and RPLC LC-MS methods in both positive and negative modes on an Agilent 6545 Q-TOF.

For validation studies of specific compound abundance, the modes identified in **Figure 3** were used. For the differential analysis, we restricted our conversation to the features extracted from C18/ESI+ using **MassHunter Explorer** for those features containing a minimum of 3000 counts (n=1423). Datasets were aligned to a pooled QC standard.For this presentation, all data in figures 7,8

Results

Samples were grouped based on the following categories:
OOC vs Organoid (ORG
Day of experient (D0/D6 for OOC, D0/D5 ORG)
Drug/Concentration (control/SN-38/STA/5-FU)
OOC Channel (Top/Bottom, Inlet/Outlet)

Initial experiments helped guide collaborators. An initial survey experiment was performed to assess the best channel for observing the drugs of interest in this study (**Figure 3**). These data were then used to confirm that drug handling (incubation/filtration) did not impact the drugs of study. SN-38 was found to be adversely impacted by degassing/filtration and SN-38 was subsequently added after degassing (**Figure 4**). There was a concern that the drugs under study could adhere to the PDMS of the OOC which we negated in **Figure 5**. Drug dosing was determined to be less efficacious in the OOC model vs traditional cell culture (**Figure 6**).

Differential metabolomics was performed on the samples in all 4 channels (currently only 1 is presented in a partially analyzed form).

There was minimal difference observed upon SN-38 and 5-FU dosing (**Figure 7**), consistent with the observation in **Figure 6**. In spite of this, there were some features identified as unique to 5-FU and SN-38 treatment (**Figure 8**). There were large disparities noted between SN-38 treatment in OOC vs ORG modalities (**Figure 9**).

Additional Findings

A throwaway observation is noted in **Figure 10** as a cautionary tale to those that simply trust m/z based identifications without validation.

Next Steps

As an apology to the reader, we are in the middle of this data analysis and look forward to in depth exploration of the 4 channels and their association to the biological impact. That said, our validations performed to this point were of value to our collaborators in the development of the OOC drug dosing study.

Acknowledgements

Funding, in part, for these efforts was provided from NIH/NCI R01CA241137 (SM PI, JK CoI).

Disclosure:
The authors have no conflicts of interest to declare.

Organ on a Chip Workflow

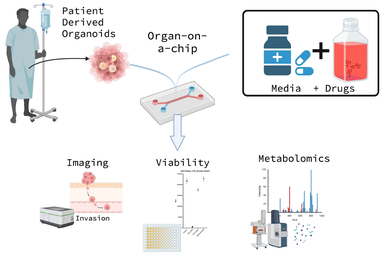

Figure 1: Patient Derived Organ on a Chip Workflow. Colorectal cancer (CRC) organoids, derived from patient tissues, were seeded onto the top channel of the Organ-on-a-Chip (OOC) device or cultured in traditional 3D plates. Both groups were subjected to chemotherapy treatment administered in CTO media. Analysis was conducted upon completion of the experiments, comparing metabolomic effluent profiles and viability between the OOC and organoids cultured on plastic.

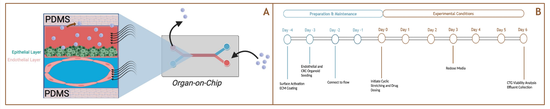

Figure 2: Organ on a Chip Platform and Timeline. A, Organ-on-chip (OOC) technology incorporates tissue compartments and mechanical forces to mimic *in vivo* peristalsis and fluid flow. Two microfluidic compartments are separated by a porous membrane, with endothelial cells in the bottom channel and patient-derived tumor organoids in the top channel. **B** shows the experimental timeline of an OOC experiment detailing dosing, effluent collection and viability analysis

Mass Spec Workflow

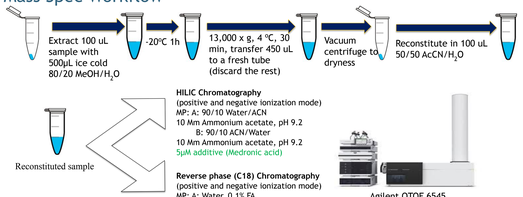

Platform Validation

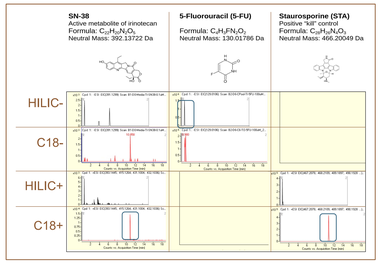

Figure 3: Compound specific LC/MS Behavior. 5-FU SN-38 and STA were run C18/HILIC ESI+/ESI- per described methods to determine the best channel for analysis. SN-38 and STA were subsequently monitored C18+ while 5-FU was monitored on HILIC-.

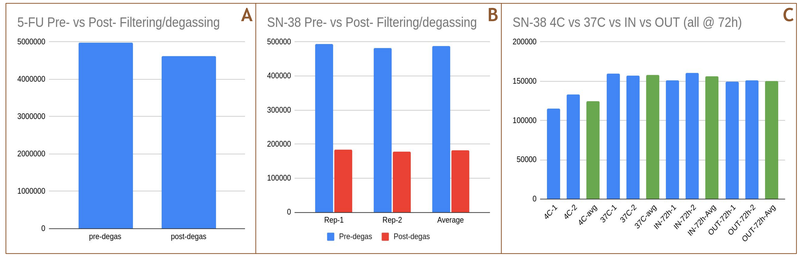

Figure 4: Impact on pre-experiment processing (filtering/temperature). In our OOC workflow, protocol includes a degassing/filtering step to remove gas ("bubbles") from solutions that will be used in the liquid reservoirs. As a precaution, 5-FU (**A**, 10 µM) and SN-38 (**B** 0.1 µM) signals were integrated from volvent samples. The loss of SN-38 was further explored to ascertain if temperature/time alone would lead to the loss of signal. As shown in C, 72h incubation (either on or off chip) at both 4 and 37 °C were not sufficient to lead to a loss of signal for SN-38. 5-FU was presumptively stable at this point (and confirmed in **Figure 5**)

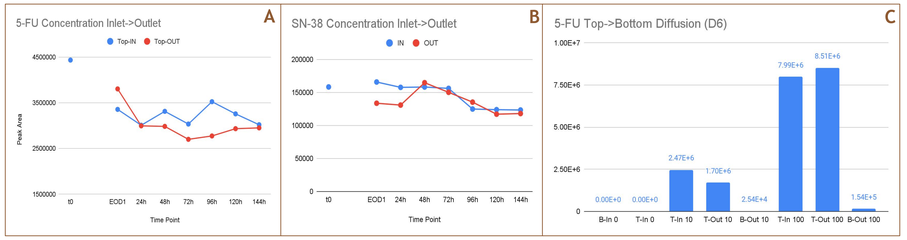

Figure 5: Confirmation of Drug/Chip Interaction. 5-FU and SN-38 show minimal interaction with the OOC Chip substrate (**A**,**B**). 5-FU shows a concentration dependant diffusion from top to bottom channel in Seeded Experiments of ~0.5% over 6 d (**C**).

5-FU (**A**, 10 µM) and SN-38 (**B**, 0.1 µM) were passed through an unseeded "blank" chip to check for PDMS binding/interaction. Shown are integrated peak areas for 5-FU and SN-38. These chips had no permeability between channels, unlike the experimental ones. The t0 point represents the media signal before being placed in a flow reservoir. The ΔSignal_in,out for the drug at equilibrium was < 20%, within the vendor's acceptable range. In panel **C**, 5-FU signals were extracted and plotted. For chip flow, reservoirs need to be filled and primed, initial variabilities and in v out discrepancies likely result from differences in these variable dilution effects.

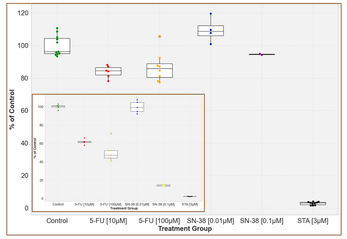

Figure 6: On Chip Confirmation of Drug Efficacy. Shown are viability, on chip, as determined by CellTiter-Glo, of the OOC seeded cells at the end of a 6 day exposure to the listed drug. Shown are the control, 5-FU, SN-38 and STA drug treatments. Note that the STA was used as a positive control for cell lethality. There was minimal effect of SN-38 and 5-FU, and within groups there was no observed dose dependant response **contrary to observed in traditional cell culture (inset)**.

Differential Analysis

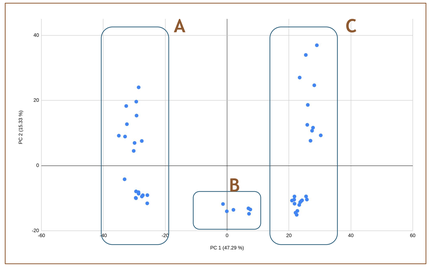

Figure 7: PCA of D6 samples separates groups into 3 categories. The C18+ samples were feature extracted at a 3000 count baseline with **Masshunter Explorer (Agilent)** yielding 1423 features. These features were used to separate the sample sets after restriction to the D6 OOC timepoints. The dominant separation was along PC1 (47.29%) yielding 3 groupings. Inspection showed that group **A** were all the non-cell controls (inlets, and bottom channel), group **B** were the outlets for the top and bottom channel of STA consistent with the observation of STA treated cells dislodging and traversing into the bottom channel. Group **C** are the outlets for the untreated, 5-FU and SN-38 treated cells; the gross level of negligible difference consistent with the observed lack of cell death (**Figure 6**).

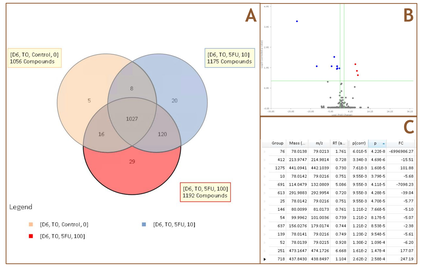

Figure 8: Feature Analysis, D6. The C18+ samples from **Figure 7** were analyzed for potential variation. Panel **A** shows a venn diagram denoting that, while most features are shared, there is a pool of ~169 features that are unique to the effluent of the 5-FU treated cells. In panel **B** we have a volcano plot showing the features enriched in the 0.1 uM treated SN-38 cells as compared to untreated (higher to the right). For completeness, the features called out as significant are shown in panel **C**. The minimal level of features is commensurate with the biological observations noted in **Figure 7** underlying the importance of tying mass spectrometric biological observations with orthogonal readouts of impact.

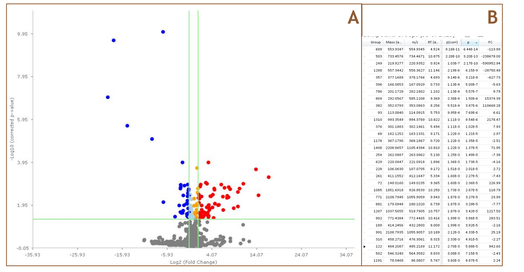

Figure 9: Exploration of the differential impact of OOC vs traditional cell culture. The C18+ samples from **Figure 7** were analyzed to explore the features of interest that might explain the differential biology as observed in **Figure 6** vs **Figure 6-Inset**. The volcano plot compares the endpoint of SN-38 treated OOC cells against the SN-38 treated organoids. Higher in OOC shown to the right (**A**). Because you would want them, the m/z, RT's of the most significant features are shown in panel (**B**).

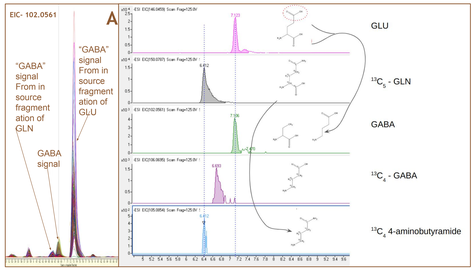

Figure 10: Spurious confounding signals from In-source decay – the need for compound validation. This figure is placed as a reminder to those new into annotation. Panel (**A**) shows an overlay (~50) of EICs from conditioned media targeting γ-aminobutyric acid (GABA). Notice the strong and proximal signals at retention times consistent with the elution of glutamate (GLU, 7.3') and glutamine (GLN, 6.6'). Panel (**B**) shows a confirmatory experiment in which a samples containing GLU, $^{13}C_5$-GLN, and $^{13}C_4$-GABA. The unlabeled peak for GABA coelutes with GLU and is presumptively generated from the GLU. While GABA signals can be generated from GLN, it is much more efficient from GLU and 4-aminobutyramide is the more commonly seen breakdown signal from GLN. This is why we have not performed putative ID's in Figures 8 and 9.

Ellison Institute of Technology
LOS ANGELES